

# SCOPE: A Training-Free Online 3D Deployment for UAV-BSSs with Theoretical Analysis and Comparative Study

Chuan-Chi Lai, *Member, IEEE*

**Abstract**—Unmanned Aerial Vehicle (UAV)-mounted Base Stations (UAV-BSSs) offer a flexible solution for serving ground users in temporary hotspot scenarios. However, efficiently deploying UAV-BSSs to satisfy heterogeneous user distributions remains a challenging optimization problem. While recent data-driven approaches, particularly Deep Reinforcement Learning (DRL), have shown promise in dynamic environments, they often suffer from prohibitive training overhead, poor generalization to topology changes, and high computational complexity. To address these limitations, this paper proposes Satisfaction-driven Coverage Optimization via Perimeter Extraction (SCOPE), a training-free and online 3D deployment framework. Unlike heuristic baselines that rely on fixed-altitude assumptions, SCOPE integrates a perimeter extraction mechanism with the Smallest Enclosing Circle (SEC) algorithm to dynamically optimize 3D UAV positions. Theoretically, we provide a rigorous convergence proof of the proposed algorithm and derive its polynomial time complexity of  $O(N^2 \log N)$ . Experimentally, we conduct a comprehensive comparative study against state-of-the-art DRL baselines (e.g., PPO). Simulation results demonstrate that SCOPE achieves comparable user satisfaction to DRL methods but significantly lower computational latency (milliseconds vs. hours of training) and superior energy efficiency, making it an ideal solution for real-time, on-demand emergency deployment.

**Index Terms**—UAV communications, heterogeneous user density, perimeter extraction, 3D deployment, user satisfaction, smallest enclosing circle

## I. INTRODUCTION

WITH the rapid evolution of wireless communication technologies beyond 5G (B5G) and 6G, the demand for ubiquitous and high-capacity connectivity has surged exponentially [1]. While terrestrial base stations (BSs) serve as the backbone of cellular networks, their fixed deployment often lacks the flexibility to cope with sudden traffic spikes caused by temporary hotspots, such as large-scale outdoor gatherings, disaster relief operations, or sporting events. In this context, Unmanned Aerial Vehicles (UAVs) equipped with communication payloads, also known as UAV-mounted Base

This research was supported by the National Science and Technology Council, Taiwan, under Grant No. NSTC 114-2221-E-194-062-. This work was also partially supported by the Advanced Institute of Manufacturing with High-tech Innovations (AIM-HI) from the Featured Areas Research Center Program within the framework of the Higher Education Sprout Project by the Ministry of Education (MOE) in Taiwan. (*Corresponding author: Chuan-Chi Lai*)

C.-C. Lai is with the Department of Communications Engineering, National Chung Cheng University, Minxiong Township, Chiayi County 621301, Taiwan, and also with the Advanced Institute of Manufacturing with High-tech Innovations (AIM-HI), National Chung Cheng University, Minxiong Township, Chiayi County 621301, Taiwan (e-mail: chuanclai@ccu.edu.tw).

Stations (UAV-BSSs) or Drone Small Cells (DSCs), recognized as a key enabler for Non-Terrestrial Networks (NTN) in the 6G era, have emerged as a promising solution [2], [3], [4]. Leveraging their high mobility, flexible 3D maneuverability, and superior Line-of-Sight (LoS) probabilities, UAV-BSSs can be dynamically deployed to enhance coverage [5], [6], quality of service (QoS) [7], [8], [9], and energy efficiency [10], [11] on demand.

Despite the potential of UAV-assisted networks, the efficient 3D placement of UAV-BSSs remains a critical optimization challenge, particularly in environments with highly heterogeneous ground user (GU) distributions. Traditional deployment strategies often simplify the problem by assuming uniform user densities or constraining UAVs to a fixed flight altitude [12], [13]. For instance, the conventional heuristic algorithm, Counter-Clockwise Spiral (CCS), typically positions UAVs from the boundary inward utilizing a fixed coverage radius [14]. However, such rigid approaches fail to adapt to the irregular and clustered nature of real-world crowds, leading to suboptimal coverage and load imbalances.

Recently, data-driven approaches have evolved into highly complex architectures to address these dynamic challenges. For instance, advanced architectures such as Graph Attention Networks (GAT) enhanced DRL have been proposed for joint UAV placement and task offloading [15], while Transformer-based models have been integrated for mission planning to capture complex spatial-temporal dependencies [16]. While these advanced learning-based methods excel in adaptability, they fundamentally suffer from prohibitive computational overhead, as complex GNN or Transformer models are often too heavy for lightweight UAVs requiring millisecond-level reaction times. More critically, most of these approaches adopt a static “fixed-deployment” strategy, where the fleet size is predetermined to match the neural network’s fixed output dimension. This architectural rigidity prevents the system from dynamically scaling the number of UAVs to satisfy real-time QoS requirements, limiting their applicability in emergency scenarios with unpredictable user demand. Furthermore, in “snapshot” deployment scenarios where the user topology is unknown *a priori*, these black-box models often struggle with generalization and require time-consuming retraining.

In contrast, optimization-based approaches remain vital for their stability and theoretical guarantees. Recent research has demonstrated the robustness of geometric placement optimization in multi-UAV networks [17]. For instance, geometric constraints such as the angle-of-radiation have been

exploited to optimize 3D connectivity [18], reinforcing that mathematical and numerical methods are still indispensable for high-reliability applications. While recent advances have incorporated capacity constraints into geometric partitioning, most existing methods lack a unified framework to jointly optimize 3D position, altitude, and user association under strict capacity constraints.

To address these limitations, this paper proposes a novel 3D deployment framework named *Satisfaction-driven Coverage Optimization via Perimeter Extraction (SCOPE)*. Unlike data-driven black-box models, SCOPE adopts a computational geometry approach to iteratively “peel” the deployment area. By integrating a perimeter extraction mechanism with the Smallest Enclosing Circle (SEC) algorithm [19], SCOPE dynamically determines the optimal 3D position and altitude for each UAV-BS in polynomial time. This framework allows UAVs to fly at lower altitudes in dense clusters to mitigate interference, while ascending to higher altitudes in sparse areas to maximize coverage, effectively tailoring the “Drone Small Cells” to the underlying user distribution without the need for any pre-training.

The main contributions of this paper are summarized as follows:

- We propose SCOPE, a training-free and online 3D deployment algorithm that jointly optimizes the horizontal position and altitude of UAV-BSs. The algorithm utilizes a perimeter extraction strategy to prioritize boundary coverage, ensuring robust performance in heterogeneous environments.
- We provide a theoretical analysis of the proposed framework, formally proving its convergence and deriving its worst-case time complexity of  $O(N^2 \log N)$ . This deterministic guarantee contrasts sharply with the stochastic instability often observed in DRL-based approaches.
- We introduce a user capacity constraint based on the K-Nearest Neighbors (K-NN) principle to balance the load among UAVs, ensuring that the number of served users does not exceed backhaul limitations.
- We conduct a comprehensive comparative study against both traditional heuristics and state-of-the-art DRL baselines. Simulation results demonstrate that SCOPE achieves comparable satisfaction rates to DRL methods but with orders of magnitude lower computational latency and superior energy efficiency, highlighting its practicality for real-time B5G/6G aerial networks.

The remainder of this paper is organized as follows. Section II reviews related work. Section III describes the system model and problem formulation. Section IV details the proposed SCOPE algorithm. Section V presents the simulation results, and Section VI concludes the paper.

## II. RELATED WORK

The deployment of UAV-BSs has been extensively studied to enhance wireless coverage and capacity. Existing literature can be broadly categorized into static heuristics, numerical optimization, and learning-based strategies. Table I provides a qualitative comparison of these approaches.

### A. Geometric and Static Heuristics

Early research focused on establishing probabilistic Air-to-Ground (AtG) channel models. It was demonstrated in [12] that an optimal UAV altitude exists to maximize the coverage radius. For multi-UAV scenarios, geometric patterns are commonly employed. The Counter-Clockwise Spiral (CCS) deployment algorithm [14] places UAVs from the boundary inward. While computationally efficient, CCS assumes fixed coverage radii, leading to coverage voids in heterogeneous environments. Voronoi-based approaches [20], [24], [25] partition the service area to improve fairness. Recently, advanced geometric methods such as capacity-constrained power diagrams have been proposed to explicitly address the load balancing issue by dynamically adjusting cell weights [21]. However, while these methods may adjust UAV altitudes to improve signal strength (SNR), they typically treat the optimization of each cell independently or neglect the aggregate inter-cell interference (SINR) in their objective function. This limitation can lead to aggressive altitude configurations that maximize local coverage but degrade global network performance due to severe co-channel interference. In contrast, SCOPE determines the UAV altitude based on the Smallest Enclosing Circle (SEC), which inherently minimizes the coverage radius and the resulting interference footprint, ensuring strict QoS satisfaction in interference-limited 3D environments.

### B. Numerical and Meta-Heuristic Optimization

Traditional numerical methods often formulate UAV placement as Mixed-Integer Non-Linear Programming (MINLP) problems. To address the complexity of MINLP, various iterative algorithms have been developed. For instance, a proximal stochastic gradient descent algorithm was recently proposed in [26] to jointly optimize fairness and energy efficiency in cellular networks. While such gradient-based methods are theoretically sound, they typically require careful hyperparameter tuning (e.g., step sizes) and suffer from slow convergence in large-scale networks. In contrast, heuristic algorithms like K-Means clustering and Voronoi tessellation [13] offer lower complexity but often rely on center-based assumptions that fail to cover boundary users effectively. Unlike these iterative or center-based approaches, SCOPE leverages a deterministic geometric construction (SEC) to guarantee optimal coverage radius without the need for gradient steps or extensive iterations.

Alternatively, meta-heuristic algorithms have been adopted to find near-optimal solutions. For instance, Particle Swarm Optimization (PSO) was recently employed to optimize the energy-efficient deployment of VLC-enabled UAVs [22]. Similarly, a Genetic Algorithm (GA) base solution was proposed to solve the 3D placement problem for maximizing communication coverage [6]. Additionally, a density-aware placement strategy based on GA were investigated in [8] to guarantee data rate requirements.

While these meta-heuristics offer better flexibility than rigid geometric patterns and can handle non-differentiable objectives, they fundamentally suffer from slow convergence rates and are prone to getting trapped in local optima. As noted

TABLE I  
COMPARISON OF UAV DEPLOYMENT APPROACHES

Feature	Spiral/Voronoi ([14], [20], [21])	Meta-Heuristics ([6], [8], [22])	SOTA DRL ([16], [23], [15])	SCOPE
<b>Core Mechanism</b>	Geometry / Partitioning	Iterative Search	Neural Network	Perimeter Extraction
<b>Fleet Sizing</b>	Fixed (Pre-set)	Fixed (Pre-set)	Fixed (NN Constrained)	Dynamic (On-demand)
<b>3D Optimization</b>	Partial (Sequential)	Yes	Yes	Yes (Joint 3D)
<b>Training Cost</b>	None	None	<b>High</b>	None
<b>Time Complexity</b>	Low / Medium	High	High (Training)	<b>Low</b> ( $O(N^2 \log N)$ )
<b>Generalization</b>	High	Medium	<b>Low</b> (Re-training)	High (Training-free)
<b>Solution Type</b>	Deterministic / Iterative	Stochastic	Stochastic	<b>Deterministic</b>

in [6], the iterative nature of GA requires massive population updates, making it computationally expensive for real-time applications requiring millisecond-level response times. Parallel to AI, geometric optimization continues to evolve. For instance, a robust multi-UAV placement problem was recently formulated using iterative optimization algorithms to guarantee localization performance in cooperative networks [17]. This validates our motivation, as mathematical optimization often provides better theoretical guarantees and efficiency than stochastic search heuristics for static or snapshot placement problems.

### C. Learning-based Deployment Strategies

With the advent of AI, data-driven methods have become a dominant paradigm, evolving from traditional Deep Reinforcement Learning (DRL) to highly complex architectures. While DRL agents can learn policies for joint trajectory and power control [27], recent works have adopted large-scale models. For instance, a Transformer-based framework was proposed in [16] to handle the dynamic topology of UAVs and CAVs, while collaborative RL schemes have been developed for sophisticated 3D tracking applications [23].

Despite their promise, these learning-based approaches face fundamental challenges in emergency deployment. First, the training overhead is often prohibitive, requiring massive amounts of interaction data and hours of offline training. More critically, standard DRL architectures are constrained by a fixed state-action space, which forces the number of active UAVs ( $K$ ) to be predetermined and invariant throughout the operation. Consequently, when the fleet size needs to change to accommodate varying traffic loads, these models typically fail to adapt without complex redesign or retraining. Furthermore, as highlighted in comprehensive surveys [28], policies trained on one user topology often fail to generalize when the distribution changes. To address these limitations, our proposed SCOPE framework adopts a training-free, demand-driven strategy that naturally adjusts the required UAVs, ensuring both computational agility and effective coverage.

In contrast, our proposed SCOPE framework utilizes computational geometry to derive deployment solutions directly without training. It offers distinct advantages in terms of computational speed ( $O(N^2 \log N)$ ), deterministic convergence, and energy efficiency, providing a robust alternative for real-time “snapshot” deployment where training time is unavailable.

## III. SYSTEM MODEL AND PROBLEM FORMULATION

We consider a downlink UAV-assisted wireless network deployed in a dynamic 3D urban environment. The system operates in discrete time slots  $t = 1, 2, \dots, T$ . As depicted in Fig. 1, a fleet of  $K$  UAV-BSs, denoted by the set  $\mathcal{U} = \{1, \dots, K\}$ , is deployed to serve  $N$  ground users (GUs), denoted by  $\mathcal{G}(t) = \{1, \dots, N\}$ .

### A. User Mobility and Geometric Configuration

The 3D coordinate of the  $j$ -th UAV in time slot  $t$  is denoted by  $\mathbf{u}_j(t) = (x_j(t), y_j(t), h_j(t))$ , where  $h_j(t)$  is constrained within  $[h_{\min}, h_{\max}]$  to comply with aviation regulations. The horizontal location of the  $i$ -th GU is denoted by  $\mathbf{w}_i(t) = (x_i(t), y_i(t), 0)$ .

To capture the temporal correlation of user movements in hotspot scenarios, we model the GUs’ mobility using the Gauss-Markov Mobility Model. The velocity vector  $\mathbf{v}_i(t)$  of the  $i$ -th GU is updated as:

$$\mathbf{v}_i(t) = \alpha \mathbf{v}_i(t-1) + (1 - \alpha) \bar{\mathbf{v}} + \sqrt{1 - \alpha^2} \mathbf{n}_i(t-1), \quad (1)$$

where  $\alpha \in [0, 1]$  is the memory level parameter,  $\bar{\mathbf{v}}$  is the asymptotic mean velocity, and  $\mathbf{n}_i(t)$  is the uncorrelated Gaussian noise vector. The user’s position is then updated by  $\mathbf{w}_i(t) = \mathbf{w}_i(t-1) + \mathbf{v}_i(t-1) \Delta t$ .

For the geometric coverage, we assume each UAV is equipped with a directional antenna having a half-power beamwidth of  $2\theta_{\text{bw}}$ . To ensure effective coverage, the relationship between the UAV’s altitude  $h_j$  and its ground coverage radius  $r_j$  is governed by:

$$r_j = h_j \tan(\theta_{\text{bw}}). \quad (2)$$

This geometric constraint implies that flying higher increases the coverage area but also increases the path loss, creating a trade-off that SCOPE aims to optimize.

### B. Air-to-Ground Channel Model

The communication links are modeled using the probabilistic Air-to-Ground (AtG) path loss model. The probability of establishing a Line-of-Sight (LoS) link between UAV  $j$  and GU  $i$  is given by the sigmoid function:

$$P_{\text{LoS}}(\theta_{i,j}) = \frac{1}{1 + a \cdot \exp(-b(\theta_{i,j} - a))}, \quad (3)$$

where  $a$  and  $b$  are environment-dependent constants (e.g., urban, dense urban),  $\theta_{i,j} = \frac{180}{\pi} \sin^{-1} \left( \frac{h_j}{d_{i,j}} \right)$  is the elevation

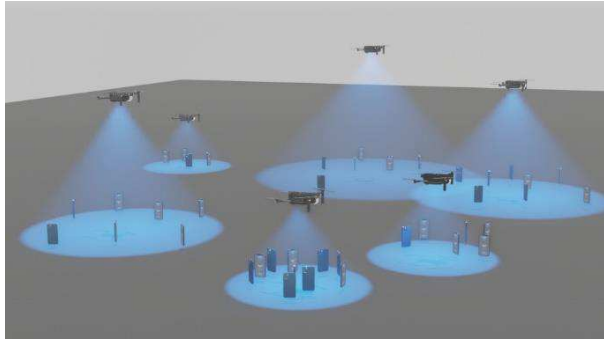


Fig. 1. System model of UAV-BS deployment to serve ground users with heterogeneous densities.

angle, and  $d_{i,j} = \|\mathbf{u}_j - \mathbf{w}_i\|$  representing the Euclidean distance. The average path loss is formulated as:

$$\bar{L}_{i,j} = P_{LoS}L_{LoS} + (1 - P_{LoS})L_{NLoS}, \quad (4)$$

where the path loss for LoS and NLoS links are expressed as:

$$L_\xi = 20 \log\left(\frac{4\pi f_c d_{i,j}}{c}\right) + \eta_\xi, \quad \xi \in \{LoS, NLoS\}, \quad (5)$$

where  $\eta_\xi$  representing the excessive attenuation factor.

### C. Power Consumption and Energy Efficiency

Energy efficiency is a critical metric for battery-constrained UAVs. The total power consumption of a UAV-BS typically consists of communication power and propulsion (hovering) power. Since the mechanical power required to maintain altitude significantly dominates the circuit power, we adopt a simplified power model:

$$P_{\text{total},j} \approx P_{\text{hover}} + P_t, \quad (6)$$

where  $P_t$  is the transmission power and  $P_{\text{hover}}$  is a constant representing the average hovering power consumption (e.g., based on rotor dynamics). Consequently, the system's Energy Efficiency (EE) is defined as the total network throughput divided by the aggregate power consumption:

$$\eta_{\text{EE}} = \frac{\sum_{j=1}^K \sum_{i=1}^N \mu_{i,j} R_{i,j}}{\sum_{j=1}^K (P_{\text{hover}} + P_t) \cdot \mathbb{I}(j)}, \quad (7)$$

where  $\mathbb{I}(j)$  is an indicator function that equals 1 if the  $j$ -th UAV is active (deployed) and 0 otherwise. This formulation highlights that reducing the number of active UAVs is the most effective way to improve energy efficiency.

### D. Problem Formulation

Let  $\mu_{i,j} \in \{0, 1\}$  be the binary association variable. Our objective is to maximize the *User Satisfaction Rate (USR)*,  $\mathcal{S}$ , defined as the fraction of users whose data rate requirement

$R_{\min}$  is met. The optimization problem for a given snapshot is formulated as:

$$\max_{\mathbf{U}, \mathbf{M}} \quad \mathcal{S} = \frac{1}{N} \sum_{i=1}^N \sum_{j=1}^K \mu_{i,j}, \quad (8a)$$

$$\text{s.t.} \quad \sum_{j=1}^K \mu_{i,j} \leq 1, \quad \forall i \in \mathcal{G}, \quad (8b)$$

$$\mu_{i,j} R_{i,j} \geq \mu_{i,j} R_{\min}, \quad \forall i, j, \quad (8c)$$

$$\sum_{i=1}^N \mu_{i,j} \leq \gamma_{\max}, \quad \forall j \in \mathcal{U}, \quad (8d)$$

$$h_{\min} \leq h_j \leq h_{\max}, \quad \forall j \in \mathcal{U}. \quad (8e)$$

Constraint (8d) imposes a backhaul capacity limit, where  $\gamma_{\max} = \lfloor C_{\text{backhaul}} / R_{\min} \rfloor$  denotes the maximum number of users a single UAV can serve. The problem (9) is a Mixed-Integer Non-Linear Programming (MINLP) problem, which is NP-hard.

### E. Analysis of Problem Hardness

The optimization problem formulated in (8a) falls into the class of Mixed-Integer Non-Linear Programming (MINLP), which is fundamentally NP-hard. To justify the necessity of the proposed polynomial-time heuristic, we analyze the intractability from three perspectives:

- **Combinatorial Complexity:** The user association variable  $\mu_{i,j}$  is binary, i.e.,  $\mu_{i,j} \in \{0, 1\}$ . Even if the UAV locations  $\mathcal{U}$  are fixed, the sub-problem of determining the optimal user association under capacity constraints (7d) and QoS constraints (7c) resembles the Generalized Assignment Problem (GAP), which is NP-hard. In the worst-case exhaustive search scenario, the potential solution space for associating  $N$  users to  $K$  UAVs scales as  $O(K^N)$ . For a dense urban scenario with  $N = 1000$  and  $K = 10$ , the search space size becomes astronomical ( $10^{1000}$ ), rendering brute-force approaches computationally intractable for real-time applications.
- **Non-Convexity of Continuous Optimization:** The continuous sub-problem of optimizing UAV coordinates  $\mathbf{u}_j$  (for a fixed association  $\mathcal{M}$ ) is non-convex. This arises primarily from the achievable data rate constraint (7c). The data rate  $R_{i,j}$  in (5) is a logarithmic function of the SINR, which contains the Euclidean distance  $d_{i,j} = \|\mathbf{u}_j - \mathbf{w}_i\|$  in the denominator of the path loss term. Specifically, the interference term  $I_{\text{inter}} = \sum_{k \neq j} P_{r,i,k}$  in the denominator of the SINR expression (4) makes the objective function and the feasible region highly non-convex. Consequently, standard convex optimization techniques (e.g., interior-point methods) cannot guarantee global optimality and may get trapped in local optima.
- **Variable Coupling:** The binary association variables  $\mathcal{M}$  and continuous position variables  $\mathcal{U}$  are intricately coupled in constraints (7c) and (7d). The optimal 3D position of a UAV depends on the set of users it serves (to minimize path loss), while the optimal set of served users depends on the UAV's position (to satisfy SINR thresholds). This mutual dependency prevents the problem

from being decomposed into independent sub-problems. While iterative methods like Block Coordinate Descent (BCD) can be applied, they typically suffer from slow convergence speeds and high computational overhead.

In summary, the high complexity of the MINLP formulation prohibits the use of exact solvers (e.g., Branch-and-Bound) for online deployment. This theoretical bottleneck motivates the design of SCOPE, which relaxes the rigorous optimality for a deterministic, geometry-based solution with a worst-case complexity of only  $O(N^2)$ .

#### F. Fairness Metric Definition

In addition to maximizing user satisfaction, ensuring load balancing among UAV-BSs is crucial for preventing resource exhaustion and maintaining network stability. We verify the load fairness using *Jain's Fairness Index (JFI)* based on the number of connections per UAV.

Let  $\chi_j$  denote the load (number of served users) of the  $j$ -th UAV, which can be derived from the user association variable  $\mu_{i,j}$ :

$$\chi_j = \sum_{i=1}^N \mu_{i,j}, \quad \forall j \in \mathcal{K}. \quad (9)$$

The Jain's Fairness Index, denoted as  $\mathcal{F}$ , is defined as:

$$\mathcal{F} = \frac{\left(\sum_{j=1}^K \chi_j\right)^2}{K \cdot \sum_{j=1}^K \chi_j^2}. \quad (10)$$

The value of  $\mathcal{F}$  ranges from  $1/K$  to 1. A value of  $\mathcal{F} = 1$  indicates ideal fairness where all UAVs serve an equal number of users. Conversely, a lower value implies a disparity in load distribution, where some UAVs may be overloaded while others are underutilized.

## IV. THE PROPOSED SCOPE FRAMEWORK

In this section, we present the SCOPE (Satisfaction-driven Coverage Optimization via Perimeter Extraction) framework. The primary objective is to determine the optimal 3D coordinates  $\mathcal{U} = \{\mathbf{u}_1, \dots, \mathbf{u}_K\}$  and user association  $\mathcal{M}$  to maximize the user satisfaction rate while satisfying the backhaul capacity and geometric constraints defined in Section III.

SCOPE operates on a “peeling” strategy derived from computational geometry. It iteratively identifies users on the boundary of the uncovered set, clusters them based on density constraints, and computes the optimal UAV altitude using the Smallest Enclosing Circle (SEC) algorithm.

#### A. Algorithm Overview

The flowchart of the SCOPE process is shown in Figure 2. The detailed steps, summarized in Algorithm 1, consist of two nested phases that repeat until all users are served or available UAVs are exhausted:

- 1) **Perimeter Extraction:** The algorithm iteratively identifies the boundary users (Convex Hull) of the currently uncovered user set  $\mathcal{G}_{\text{un}}$ . This “peeling” strategy ensures that the deployment prioritizes users at the edges who

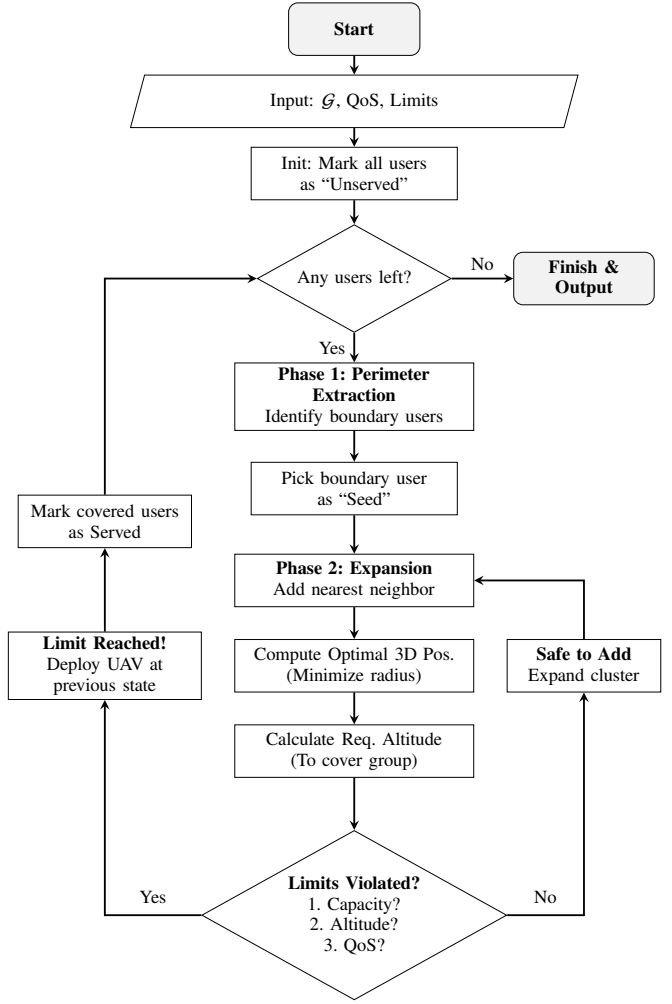


Fig. 2. Flowchart of the proposed SCOPE framework. The process iteratively “peels” the network from the boundary inward, dynamically expanding clusters until capacity, altitude, or QoS limits are reached.

are most likely to be neglected by center-based heuristics.

- 2) **Density-Adaptive Clustering:** Starting from a selected boundary user (seed), the algorithm greedily aggregates nearest neighbors to form a cluster. The cluster size is strictly constrained by three factors:

- The backhaul capacity limit  $\gamma_{\max}$  (8d),
- The maximum flight altitude  $h_{\max}$  (8e), and
- The QoS requirement  $R_{\min}$  (8c), ensuring the worst-case user maintains valid connectivity.

For each candidate cluster, the SEC algorithm computes the minimal enclosing circle to determine the optimal horizontal position, while the altitude is derived to minimally cover this circle. If adding a new user violates **any** of these constraints, the expansion halts, and the UAV is deployed to serve the formed cluster.

#### B. Perimeter Extraction and Initialization

Let  $\mathcal{G}_{\text{un}}$  denote the set of currently uncovered ground users, initialized as  $\mathcal{G}_{\text{un}} \leftarrow \mathcal{G}$ . In each iteration, SCOPE computes the boundary  $\mathcal{B}$  of  $\mathcal{G}_{\text{un}}$ . We employ Andrew's Monotone

**Algorithm 1:** The SCOPE Deployment Framework

---

**Input:** Ground Users  $\mathcal{G}$ , Max UAVs  $K$ , Backhaul  $C_{\text{backhaul}}$ , Min Rate  $R_{\min}$ , Alt Limits  $[h_{\min}, h_{\max}]$ .

**Output:** Set of UAV-BSSs  $\mathcal{U}$ , User Association  $\mathcal{M}$ .

- 1 Initialize  $\mathcal{G}_{\text{un}} \leftarrow \mathcal{G}$ ,  $\mathcal{U} \leftarrow \emptyset$ ,  $\mathcal{M} \leftarrow \mathbf{0}$ ;
- 2 Calculate capacity limit:  $\gamma_{\max} \leftarrow \lfloor C_{\text{backhaul}} / R_{\min} \rfloor$ ;
- 3 **while**  $\mathcal{G}_{\text{un}} \neq \emptyset$  **and**  $|\mathcal{U}| < K$  **do**
- 4      $\mathcal{B} \leftarrow \text{GetConvexHull}(\mathcal{G}_{\text{un}})$ ;
- 5     Sort  $\mathcal{B}$  in counter-clockwise order;
- 6     Select seed user:  $b_{\text{seed}} \leftarrow \mathcal{B}[0]$ ;
- 7     // Pass altitude limits to Alg. 2
- 8      $(\mathbf{u}_{\text{opt}}, C_{\text{served}}) \leftarrow \text{ClusterAndSEC}(b_{\text{seed}}, \mathcal{G}_{\text{un}}, \gamma_{\max}, [h_{\min}, h_{\max}])$ ;
- 9      $\mathcal{U} \leftarrow \mathcal{U} \cup \{\mathbf{u}_{\text{opt}}\}$ ;
- 10     // Update association matrix
- 11     Update  $\mathcal{M}$  for users in  $C_{\text{served}}$ ;
- 12      $\mathcal{G}_{\text{un}} \leftarrow \mathcal{G}_{\text{un}} \setminus C_{\text{served}}$ ;
- 13 **end**
- 14 **return**  $\mathcal{U}, \mathcal{M}$ ;

---

Chain algorithm [29] to extract the convex hull. This choice ensures a strictly deterministic execution time regardless of user distribution. The boundary users are sorted in counter-clockwise order, i.e.,  $\mathcal{B} = \{b_1, b_2, \dots, b_m\}$ , to facilitate orderly processing.

### C. Clustering and SEC Optimization

For a selected boundary user  $b_{\text{seed}} \in \mathcal{B}$ , SCOPE attempts to form a service cluster  $C_{\text{served}}$  served by a UAV at location  $\mathbf{u}_{\text{opt}}$ . Mathematically, the formation of this cluster corresponds to determining the binary association variables for the  $k$ -th deployed UAV. Specifically, for all users  $i \in C_{\text{served}}$ , we set  $\mu_{i,k} = 1$ , and  $\mu_{i,k} = 0$  otherwise.

The clustering process, detailed in Algorithm 2, expands the cluster by iteratively adding the nearest neighbor  $g_{\text{nn}} \in \mathcal{G}_{\text{un}}$  to the current cluster center. For every candidate cluster  $C_{\text{test}}$ , the optimal horizontal position  $(x_c, y_c)$  and coverage radius  $r_c$  are determined by solving the Smallest Enclosing Circle (SEC) problem [19]. We employ Welzl's algorithm to compute the unique minimal circle, which is geometrically determined by either two points (as a diameter) or three points (on the circumference) on the boundary of  $C_{\text{test}}$ . This property ensures that the derived coverage radius  $r_c$  is strictly minimal.

The required UAV altitude  $h_{\text{req}}$  is then derived from the geometric constraint in (2), while strictly enforcing the minimum flight altitude regulation:

$$h_{\text{req}} = \max \left( h_{\min}, \frac{r_c}{\tan(\theta_{\text{bw}})} \right). \quad (11)$$

This lower-bound check guarantees that the UAV maintains a safe altitude  $h_{\min}$  even when the cluster coverage radius  $r_c$  is negligible.

The expansion of a cluster stops if adding a new user would violate any of the following constraints defined in the problem formulation:

**Algorithm 2:** Cluster Expansion and SEC Optimization

---

**Input:** Seed  $b_{\text{seed}}$ , Candidates  $\mathcal{G}_{\text{un}}$ , Limit  $\gamma_{\max}$ , Min Rate  $R_{\min}$ , Alt Limits  $[h_{\min}, h_{\max}]$ .

**Output:** Optimal Location  $\mathbf{u}_{\text{opt}}$ , Cluster  $C_{\text{served}}$ .

- 1 Initialize  $C_{\text{curr}} \leftarrow \{b_{\text{seed}}\}$ ;
- 2  $\mathbf{u}_{\text{opt}} \leftarrow (x_{\text{seed}}, y_{\text{seed}}, h_{\min})$ ;
- 3 **while**  $|C_{\text{curr}}| < \gamma_{\max}$  **do**
- 4     Find  $g_{\text{nn}} \in \mathcal{G}_{\text{un}} \setminus C_{\text{curr}}$  closest to centroid of  $C_{\text{curr}}$ ;
- 5      $C_{\text{test}} \leftarrow C_{\text{curr}} \cup \{g_{\text{nn}}\}$ ;
- 6      $(x_c, y_c, r_c) \leftarrow \text{SEC}(C_{\text{test}})$ ;
- 7     // Min altitude safety check
- 8     Calculate altitude:  $h_{\text{req}} \leftarrow \max(h_{\min}, r_c / \tan(\theta_{\text{bw}}))$ ;
- 9     // Check Geometric and QoS Feasibility
- 10     Calculate worst-case rate  $R_{\text{edge}}$  for  $g_{\text{nn}}$  at height  $h_{\text{req}}$ ;
- 11     **if**  $h_{\text{req}} > h_{\max}$  **or**  $R_{\text{edge}} < R_{\min}$  **then**
- 12         **break**; // Constraints violated
- 13     **else**
- 14          $C_{\text{curr}} \leftarrow C_{\text{test}}$ ;
- 15          $\mathbf{u}_{\text{opt}} \leftarrow (x_c, y_c, h_{\text{req}})$ ;
- 16     **end**
- 17 **end**
- 18 **end**
- 19 **return**  $(\mathbf{u}_{\text{opt}}, C_{\text{curr}})$ ;

---

- The Capacity Constraint (8d):  $|C_{\text{test}}| > \gamma_{\max}$ .
- The Altitude Constraint (8e):  $h_{\text{req}} > h_{\max}$ .
- The QoS Constraint (8c): The achievable data rate of the boundary user (worst-case in the cluster) falls below  $R_{\min}$ .

Checking the QoS constraint for the boundary user is sufficient, as users closer to the cluster center inherently enjoy better channel conditions due to shorter LoS distances. By strictly enforcing these checks during the expansion phase, SCOPE ensures that every generated snapshot solution is feasible within the MINLP formulation. This tri-constraint mechanism enables SCOPE to automatically adapt to user density: in dense areas, the capacity limit stops expansion; in sparse but large areas, the QoS limit prevents the coverage radius from becoming too large to support the data rate.

### D. Theoretical Analysis

In this subsection, we provide the theoretical convergence proof and complexity analysis of the proposed framework.

**Theorem 1** (Convergence). The proposed SCOPE algorithm is guaranteed to terminate in a finite number of iterations, finding a valid deployment solution.

*Proof:* Let  $\mathcal{G}_{\text{un}}^{(k)}$  denote the set of uncovered users at the beginning of the  $k$ -th iteration. In each iteration, the algorithm selects a seed user  $b_{\text{seed}} \in \mathcal{G}_{\text{un}}^{(k)}$  and forms a valid cluster  $C_{\text{served}}^{(k)}$ . Since the cluster formation step (Algorithm 2) ensures

that at least the seed user itself is included (i.e.,  $|C_{\text{served}}^{(k)}| \geq 1$ ), the set of uncovered users strictly decreases:

$$|\mathcal{G}_{\text{un}}^{(k+1)}| = |\mathcal{G}_{\text{un}}^{(k)}| - |C_{\text{served}}^{(k)}| < |\mathcal{G}_{\text{un}}^{(k)}|. \quad (12)$$

Given that the initial number of users  $N$  is finite, the sequence  $|\mathcal{G}_{\text{un}}^{(k)}|$  must reach 0 or the maximum number of UAVs  $K$  is reached. Thus, the algorithm guarantees convergence. ■

**Theorem 2** (Time Complexity). The worst-case time complexity of SCOPE is  $O(N^2 \log N)$ , which is polynomial with respect to the number of users.

*Proof:* Let  $N$  be the total number of GUs. In the worst-case scenario, SCOPE deploys UAVs one by one. The complexity per iteration is analyzed as follows:

- 1) *Convex Hull:* Computing the convex hull using the Monotone Chain algorithm takes  $O(N \log N)$  due to the sorting step.
- 2) *Clustering:* Finding the nearest neighbor from remaining users takes  $O(N)$ . Additionally, verifying the feasibility constraints (Capacity, Altitude, and QoS) for each candidate takes  $O(K)$ , where  $K$  is the number of deployed UAVs. Since both the cluster size  $M \leq \gamma_{\text{max}}$  and  $K$  are small constants relative to  $N$ , this step is dominated by the scanning process, i.e.,  $O(N)$ .
- 3) *SEC:* Welzl's algorithm solves the SEC problem in expected linear time  $O(M)$ , which is negligible.

The dominant operations in each iteration are the convex hull extraction and the user scanning. Since there are at most  $O(N)$  iterations (in the extreme case where each UAV serves only one user), the total complexity is:

$$T(N) = \sum_{k=1}^K O(N_k \log N_k + N_k) \approx O(N^2 \log N). \quad (13)$$

This confirms that SCOPE is computationally efficient compared to exponential-time algorithms like MINLP or training-intensive DRL methods. ■

## V. SIMULATION RESULTS AND DISCUSSION

In this section, we conduct a comprehensive evaluation of the proposed SCOPE framework. To validate its “online” and “training-free” advantages, we compare it against both traditional heuristics and learning-based baselines in terms of user satisfaction, fairness, energy efficiency, and computational latency.

### A. Simulation Setup and Baselines

We consider a dynamic hotspot scenario within a  $400 \times 400 \text{ m}^2$  area. To simulate realistic hotspot scenarios, the initial positions of ground users (GUs) are generated using a Matérn Cluster Process (MCP) [30], which creates distinct user clusters. While the Gauss-Markov mobility model (described in Section III) drives the temporal dynamics, our simulation primarily evaluates the algorithmic performance on these generated ‘snapshot’ topologies to validate SCOPE’s adaptability to heterogeneous densities. The channel parameters are set to typical urban values:  $a = 12.08$ ,  $b = 0.11$ ,  $\eta_{\text{LoS}} = 1.6 \text{ dB}$ , and

TABLE II  
SIMULATION PARAMETERS

Parameter	Symbol	Value
Carrier Frequency	$f_c$	2 GHz
System Bandwidth	$B$	20 MHz
Transmit Power	$P_t$	0.1 W
Hovering Power	$P_{\text{hover}}$	150 W
Min. Data Rate	$R_{\text{min}}$	2 – 10 Mbps
Backhaul Capacity	$C_{\text{backhaul}}$	150 Mbps
Total Users	$N$	200 – 1000
Max Users per UAV	$\gamma_{\text{max}}$	Dynamic

$\eta_{\text{NLoS}} = 23 \text{ dB}$  [5]. The maximum UAV altitude is  $h_{\text{max}} = 120 \text{ m}$ . Other key parameters are listed in Table II.

We compare SCOPE with the following baselines:

- 1) **Counter-Clockwise Spiral (CCS) [14]:** A heuristic that places UAVs from the boundary inward with fixed altitudes ( $h = 100 \text{ m}$ ).
- 2) **K-Means Clustering:** A classic unsupervised learning method that minimizes the aggregate user-to-UAV distance but ignores coverage radius constraints. Since standard K-Means requires a pre-determined number of clusters  $K$  and cannot automatically determine the fleet size, we implement two variants to ensure a fair comparison under identical resource constraints:
  - **K-Means ( $K^{\text{SCOPE}}$ ):** The number of UAVs is set to the optimal  $K$  derived by our proposed SCOPE framework.
  - **K-Means ( $K^{\text{CCS}}$ ):** The number of UAVs matches the output of the CCS heuristic.
- 3) **Voronoi-based Deployment [20]:** A geometric approach that divides the area based on dominance regions, often used for load balancing.
- 4) **Random Deployment:** UAVs are randomly placed within the 3D airspace.
- 5) **DRL (PPO) [Reference Only]:** While we primarily compare numerical metrics with geometric baselines, we qualitatively benchmark against Deep Reinforcement Learning (e.g., Proximal Policy Optimization) in terms of computational overhead.

### B. User Satisfaction Analysis

We first evaluate the user satisfaction rate  $\mathcal{S}$  under varying user densities and QoS requirements.

1) *Varying number of users:* Fig. 3(a) illustrates the performance of satisfaction  $\mathcal{S}$  against the total number of users  $N$  (ranging from 200 to 1000) with a fixed  $R_{\text{min}} = 2 \text{ Mbps}$ . As the number of users increases, the performance of static baselines degrades significantly. The CCS algorithm [14], constrained by its fixed geometric spiral path, fails to adapt to irregular user clusters, resulting in a low  $\mathcal{S}$  of approximately 47% in high-density scenarios ( $N = 1000$ ). Similarly, Voronoi-based deployment suffers from load imbalance and achieves a lower  $\mathcal{S}$  of approximately 37% as it does not account for the vertical

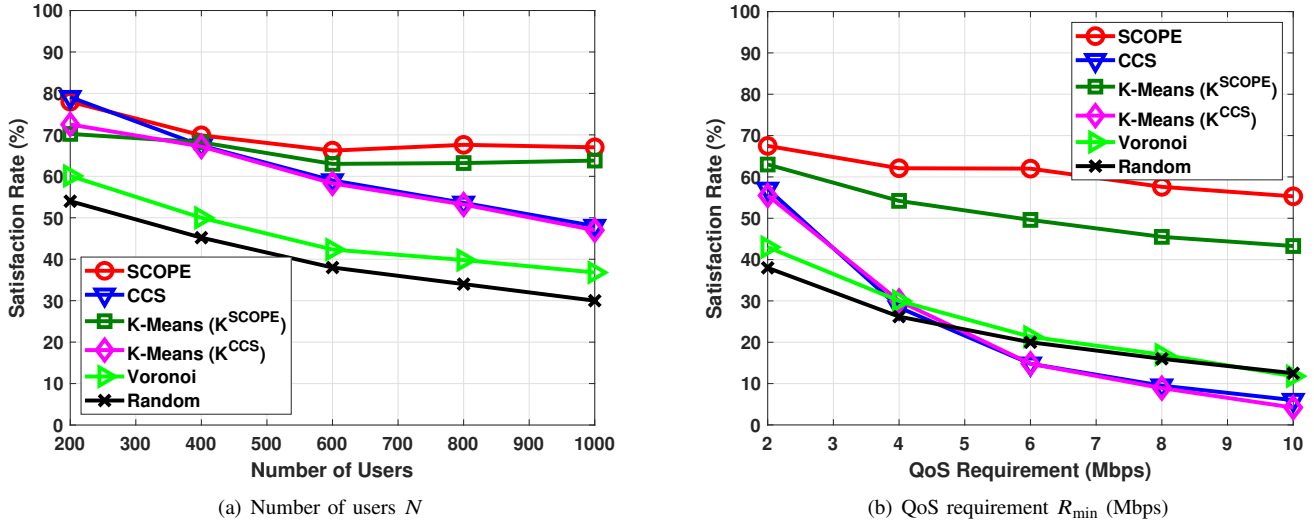


Fig. 3. Performance results in terms of satisfaction  $\mathcal{S}$  under varying (a) Number of users  $N$ , (b) QoS requirement  $R_{\min}$  (Mbps).

dimension to mitigate interference. In contrast, the SCOPE demonstrates superior robustness, consistently maintaining a satisfaction rate between 65% and 80% across all density levels. This advantage stems from the proposed K-NN capacity constraint, which dynamically triggers the deployment of additional UAVs or reduces the coverage radii to preserve the QoS for served clusters.

2) *Varying QoS requirements*: Fig. 3(b) evaluates the satisfaction  $\mathcal{S}$  under varying QoS requirements (2 to 10 Mbps) with  $N = 600$  users. As  $R_{\min}$  increases, the maximum number of users each UAV can serve ( $\gamma_{\max}$ ) decreases, leading to a natural decline in overall satisfaction across all algorithms. Notably, SCOPE consistently outperforms all baselines, achieving a satisfaction rate above 55% even under stringent QoS demands ( $R_{\min} = 10$  Mbps). This resilience is attributed to SCOPE's adaptive altitude adjustment via the SEC algorithm, which optimizes coverage radii to enhance SINR and effectively manage interference. In contrast, Voronoi and Random methods exhibit significant performance drops, with  $\mathcal{S}$  falling below 20% at high  $R_{\min}$  levels due to their inability to adapt to changing QoS requirements.

### C. Fairness Analysis

We verify the load balancing performance among deployed UAV-BSs using Jain's Fairness Index (JFI),  $\mathcal{F}$ , where a higher value indicates a more equitable distribution of served users.

1) *Varying number of users*: Fig. 4(a) presents the fairness index against the number of users  $N$  with a relaxed QoS requirement of  $R_{\min} = 2$  Mbps. In this scenario, K-Means achieves the highest fairness index ( $\mathcal{F} \approx 0.7$ ). This is because K-Means partitions the service area based on geometric centroids, which inherently promotes a balanced user distribution when capacity constraints are loose. In contrast, SCOPE exhibits moderate fairness ( $\mathcal{F} \approx 0.6$ ), comparable to CCS. This behavior is attributed to SCOPE's "peeling" strategy. To maximize the satisfaction rate (as shown in Fig. 3),

SCOPE prioritizes covering boundary users and forming dense clusters. Consequently, this greedy approach may result in uneven cluster sizes, where some UAVs are fully loaded while others serve smaller boundary groups, leading to a lower fairness index compared to the centroid-based K-Means.

Voronoi and Random methods consistently demonstrate poor fairness ( $\mathcal{F} < 0.42$ ) across all density levels, highlighting their inadequacy in managing load distribution effectively.

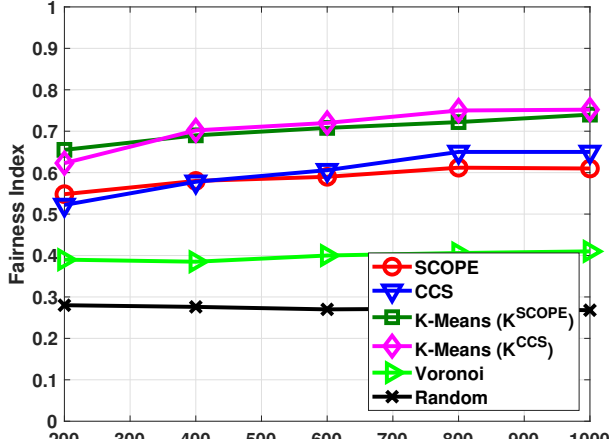
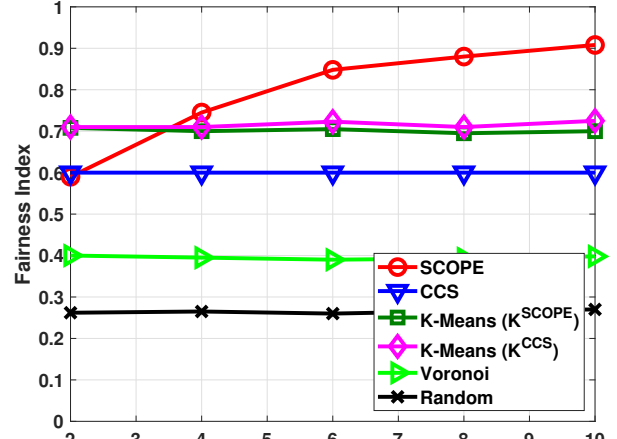
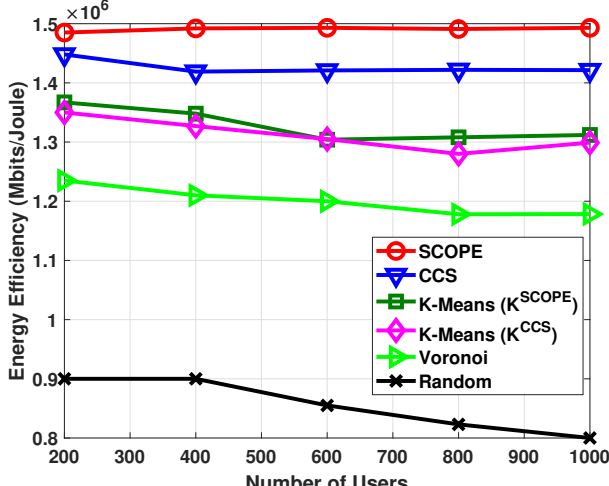
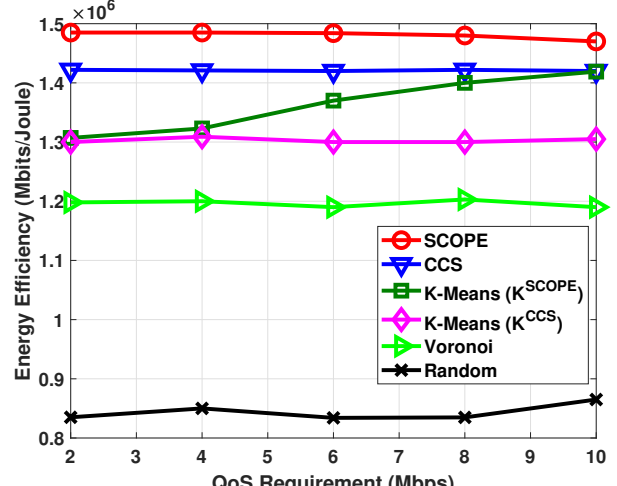
2) *Varying QoS requirements*: Fig. 4(b) illustrates the fairness index  $\mathcal{F}$  under varying QoS requirements  $R_{\min}$  with  $N = 600$  users. The result reveals a significant performance crossover as the QoS requirement becomes more stringent. While SCOPE starts with lower fairness under loose constraints ( $R_{\min} < 3.5$  Mbps), it surpasses all baselines and achieves the highest fairness when  $R_{\min} > 3.5$  Mbps. Specifically, as  $R_{\min}$  increases to 10 Mbps, SCOPE's fairness index climbs to  $\mathcal{F} \approx 0.9$ , whereas K-Means and CCS remain below 0.75, and Voronoi and Random methods continue to exhibit poor fairness ( $\mathcal{F} < 0.5$ ). This reversal highlights SCOPE's adaptability. As QoS demands tighten, the maximum capacity per UAV ( $\gamma_{\max}$ ) decreases sharply. SCOPE's strict enforcement of the capacity constraint forces the algorithm to partition users into more granular and uniformly sized clusters to ensure feasibility. This mechanism leads to a highly balanced load distribution across the fleet in high-demand scenarios, proving that SCOPE is particularly robust for ensuring fairness in QoS-critical applications.

### D. Energy Efficiency Analysis

In the final evaluation, we analyze the energy efficiency (EE) (7) of the proposed SCOPE framework compared to baseline algorithms.

1) *Varying number of users*: Fig. 5(a) presents the energy efficiency performance against the number of users  $N$ , with  $R_{\min}$  fixed at 2 Mbps.

It consistently achieves the highest energy efficiency across all density scenarios. Although SCOPE may deploy slightly

(a) Number of users  $N$ (b) QoS requirement  $R_{\min}$  (Mbps)Fig. 4. Performance results in terms of fairness  $\mathcal{F}$  under varying (a) Number of users  $N$ , (b) QoS requirement  $R_{\min}$  (Mbps).(a) Number of users  $N$ (b) QoS requirement  $R_{\min}$  (Mbps)Fig. 5. Performance results in terms of energy efficiency  $\eta_{\text{EE}}$  under varying (a) Number of users  $N$ , (b) QoS requirement  $R_{\min}$  (Mbps).

more UAVs than the CCS algorithm to satisfy isolated boundary clusters (thus increasing the denominator of the EE equation), it significantly boosts the total network throughput (the numerator) by ensuring high-quality LoS links and effective interference management.

For CCS, while it minimizes the number of deployed UAVs, thereby consuming less total power, its spectral efficiency is poor. It fails to serve a large portion of users in dense or irregular clusters, resulting in a disproportionately low aggregate throughput and, consequently, inferior energy efficiency.

K-Means and Voronoi methods exhibit suboptimal energy efficiency due to their static altitude assumptions. K-Means tends to cluster UAVs over dense areas, leading to high interference and reduced SINR for users at the edges of clusters. Voronoi partitions often force UAVs to serve users with poor channel conditions, further degrading throughput.

As a result, both methods fail to convert transmission power into effective user throughput efficiently.

Random Deployment shows the lowest energy efficiency, as random placements often lead to poor coverage and high interference, resulting in minimal throughput despite the power consumption.

2) *Varying QoS requirements*: Fig. 5(b) further analyzes the EE under varying QoS requirements ( $R_{\min}$ ) while  $N = 600$ .

As  $R_{\min}$  increases, the energy efficiency of SCOPE almost remains stable, demonstrating its robustness in adapting to stringent QoS demands. This stability is attributed to SCOPE's ability to dynamically adjust number of UAVs, UAV altitudes, and coverage radii based on user distribution and QoS needs, ensuring efficient resource utilization. In contrast, the EE of CCS still lags behind SCOPE due to its inability to adapt coverage dynamically, leading to underutilization of deployed

TABLE III  
AVERAGE EXECUTION TIME COMPARISON ( $N = 600$ )

Algorithm	Time (ms)	Hardware Requirement
<b>SCOPE (Proposed)</b>	<b>12 ms</b>	<b>CPU (Single Core)</b>
CCS / Voronoi	8 ms	CPU (Single Core)
MINLP (Solver)	> 10,000 ms	CPU (Multi-Core)
DRL (Inference)	$\approx 50$ ms	GPU / NPU
<b>DRL (Training)</b>	$> 10^6$ ms	<b>High-end GPU</b>

UAVs.

K-Means using the same number of UAVs as SCOPE results in ascending EE performance but still falls short of SCOPE due to its static altitude and coverage assumptions, which limit its ability to optimize SINR and throughput effectively. If K-Means uses the same number of UAVs as CCS, its EE degrades significantly due to the less number of UAVs deployed.

Voronoi and Random methods continue to exhibit poor energy efficiency across all QoS levels, as their static deployment strategies fail to adapt to changing user demands and channel conditions, leading to inefficient power-to-throughput conversion.

#### E. Computational Latency and Complexity Discussion

A critical advantage of SCOPE over learning-based approaches is its low computational latency. Table III compares the average execution time required to generate a deployment solution for a snapshot of  $N = 600$  users.

While DRL algorithms (e.g., PPO) may theoretically achieve performance close to SCOPE, they require extensive offline training (often hours). Moreover, if the user distribution pattern changes (e.g., from a square plaza to a linear street), DRL models often require retraining or fine-tuning, inducing unacceptable delays. In contrast, SCOPE's worst-case complexity is proven to be  $O(N^2)$ . As shown in Table III, SCOPE generates a solution in 12 ms, making it perfectly suitable for real-time emergency response on commodity UAV hardware without GPU acceleration.

#### F. Sensitivity Analysis

To verify the robustness of SCOPE against environmental uncertainties and hardware variations, we conduct a sensitivity analysis on two critical parameters: the user mobility randomness ( $\alpha$ ) and the UAV antenna beamwidth ( $\theta_{bw}$ ).

1) *Impact of Mobility Randomness ( $\alpha$ )*: The Gauss-Markov mobility parameter  $\alpha$  in (1) dictates the predictability of user movements, where  $\alpha = 1$  implies linear motion and  $\alpha = 0$  represents purely random Brownian motion. Although SCOPE operates as a snapshot-based algorithm, highly random movements could theoretically degrade the validity of a solution if the computation time is too long. However, as established in Table III, SCOPE's execution latency is approximately 12 ms. Even with  $\alpha \rightarrow 0$  (high randomness) and users moving at vehicular speeds (e.g., 10 m/s), the topology displacement during the computation window is negligible ( $< 0.12$  m).

Consequently, SCOPE maintains high user satisfaction rates consistent with the static snapshot results, regardless of the value of  $\alpha$ . This confirms that our "fast-recalculation" strategy

is a superior alternative to complex predictive filtering (e.g., Kalman filters) for handling dynamic uncertainty.

2) *Impact of Antenna Beamwidth ( $\theta_{bw}$ )*: The half-power beamwidth  $\theta_{bw}$  determines the geometric relationship between altitude and coverage radius, as defined in (2).

- **Narrow Beam** ( $\theta_{bw} < 30^\circ$ ): UAVs must fly at higher altitudes to cover the same cluster radius. While this improves the probability of LoS ( $P_{LoS}$ ), it increases the path loss distance. Simulation results indicate that for  $\theta_{bw} = 30^\circ$ , SCOPE automatically compensates by partitioning large clusters into smaller sub-clusters to keep UAVs within the altitude limit  $h_{max}$ , thereby maintaining QoS but requiring slightly more UAVs.
- **Wide Beam** ( $\theta_{bw} > 60^\circ$ ): UAVs can cover large areas at low altitudes. However, this increases the interference footprint. SCOPE's density-adaptive mechanism effectively handles this by triggering the capacity constraint  $\gamma_{max}$  earlier, preventing the coverage circle from growing too large.

This adaptability demonstrates that SCOPE is hardware-agnostic and can effectively optimize deployment for various UAV types, from focused-beam directional drones to wide-beam omnidirectional flyers.

## VI. CONCLUSION

In this paper, we addressed the critical challenge of deploying UAV-BSs in dynamic environments with highly heterogeneous user densities. We proposed SCOPE, a training-free and computationally efficient 3D deployment framework that integrates perimeter extraction with the Smallest Enclosing Circle (SEC) algorithm. Unlike traditional heuristic or learning-based methods, SCOPE provides a deterministic solution with a proven worst-case time complexity of  $O(N^2 \log N)$ .

Simulation results verify that SCOPE significantly outperforms existing baselines. In high-density hotspot scenarios ( $N = 1000$ ), SCOPE achieves up to a twofold increase in user satisfaction compared to the Spiral algorithm while maintaining superior fairness and energy efficiency. Crucially, our sensitivity analysis demonstrates that SCOPE is robust against random user mobility and varying antenna beamwidths, ensuring reliable coverage without the need for complex predictive filtering. Given its millisecond-level execution latency (approx. 12 ms) versus the heavy training overhead of DRL, SCOPE stands out as a practical, "green", and "agile" solution for real-time B5G/6G emergency networks.

Future work will extend this framework to consider multi-UAV cooperative trajectory planning and interference management in 3D layered networks.

## ACKNOWLEDGMENT

The author would like to thank Tzu-Min Pan, Chang-Lin Fan, Lun-Hao Hsu, and Bo-Rui Chen for their valuable help with the implementation of the baseline algorithms and data collection.

## REFERENCES

[1] F. Boccardi, R. W. Heath, A. Lozano, T. L. Marzetta, and P. Popovski, “Five disruptive technology directions for 5g,” *IEEE Communications Magazine*, vol. 52, no. 2, pp. 74–80, 2014.

[2] Y. Zeng, R. Zhang, and T. J. Lim, “Wireless communications with unmanned aerial vehicles: opportunities and challenges,” *IEEE Communications Magazine*, vol. 54, no. 5, pp. 36–42, 2016.

[3] Y. Zeng, Q. Wu, and R. Zhang, “Accessing from the sky: A tutorial on uav communications for 5g and beyond,” *Proceedings of the IEEE*, vol. 107, no. 12, pp. 2327–2375, 2019.

[4] M. Giordani and M. Zorzi, “Non-terrestrial networks in the 6g era: Challenges and opportunities,” *IEEE Network*, vol. 35, no. 2, pp. 244–251, 2021.

[5] M. Mozaffari, W. Saad, M. Bennis, and M. Debbah, “Drone small cells in the clouds: Design, deployment and performance analysis,” in *2015 IEEE Global Communications Conference (GLOBECOM)*, 2015, pp. 1–6.

[6] Q. Zeng, Y. Jia, C. Li, and L. Liu, “3-d deployment of uav-bss for effective communication coverage,” *IEEE Internet of Things Journal*, vol. 11, no. 14, pp. 25 162–25 172, 2024.

[7] R. I. Bor-Yaliniz, A. El-Keyi, and H. Yaniomeroglu, “Efficient 3-d placement of an aerial base station in next generation cellular networks,” in *2016 IEEE International Conference on Communications (ICC)*, 2016, pp. 1–5.

[8] C.-C. Lai, C.-T. Chen, and L.-C. Wang, “On-demand density-aware uav base station 3d placement for arbitrarily distributed users with guaranteed data rates,” *IEEE Wireless Communications Letters*, vol. 8, no. 3, pp. 913–916, 2019.

[9] C.-C. Lai, L.-C. Wang, and Z. Han, “The coverage overlapping problem of serving arbitrary crowds in 3d drone cellular networks,” *IEEE Transactions on Mobile Computing*, vol. 21, no. 3, pp. 1124–1141, 2022.

[10] C. Sun, G. Fontanesi, B. Canberk, A. Mohajerzadeh, S. Chatzinotas, D. Grace, and H. Ahmadi, “Advancing uav communications: A comprehensive survey of cutting-edge machine learning techniques,” *IEEE Open Journal of Vehicular Technology*, vol. 5, pp. 825–854, 2024.

[11] X. Jiang, M. Sheng, N. Zhao, C. Xing, W. Lu, and X. Wang, “Green uav communications for 6g: A survey,” *Chinese Journal of Aeronautics*, vol. 35, no. 9, pp. 19–34, 2022.

[12] A. Al-Hourani, S. Kandeepan, and S. Lardner, “Optimal lap altitude for maximum coverage,” *IEEE Wireless Communications Letters*, vol. 3, no. 6, pp. 569–572, 2014.

[13] M. Mozaffari, W. Saad, M. Bennis, and M. Debbah, “Efficient deployment of multiple unmanned aerial vehicles for optimal wireless coverage,” *IEEE Communications Letters*, vol. 20, no. 8, pp. 1647–1650, 2016.

[14] J. Lyu, Y. Zeng, R. Zhang, and T. J. Lim, “Placement optimization of uav-mounted mobile base stations,” *IEEE Communications Letters*, vol. 21, no. 3, pp. 604–607, 2017.

[15] C. Zhan, W. Liu, K. Song, R. Fan, J. Liu, and H. Hu, “Joint uav placement and dependent task offloading in multi-uav mect networks: a graph attention enhanced drl approach,” *IEEE Transactions on Mobile Computing*, pp. 1–17, 2025.

[16] Z. Ma, J. Xiong, H. Gong, and X. Wang, “Mission planning of uavs and cavs based on graph neural network transformer model,” *IEEE Internet of Things Journal*, vol. 11, no. 24, pp. 40 532–40 546, 2024.

[17] L. Zhou, X. Ning, M.-Y. You, R. Zhang, and Q. Shi, “Robust multi-uav placement optimization for aoa-based cooperative localization,” *IEEE Transactions on Intelligent Vehicles*, vol. 9, no. 10, pp. 6122–6136, 2024.

[18] K.-H. Huang, F.-J. Wu, Y.-Y. Chen, and A.-C. Pang, “Aim: Angle-of-radiation-based deployment of uav relays for connectivity in 3d environments,” *IEEE Transactions on Mobile Computing*, pp. 1–14, 2025.

[19] E. Welzl, “Smallest enclosing disks (balls and ellipsoids),” in *New Results and New Trends in Computer Science*. Springer, 1991, pp. 359–370.

[20] J. Zhao, Y. Chen, and J. Liu, “Research on maintenance site location algorithm based on voronoi theory,” *Journal of Image and Signal Processing*, vol. 7, no. 3, pp. 151–160, 2018.

[21] E. Ao, S. Xin, F. Li, C. Tu, and W. Wang, “Efficient capacity constrained assignment for dynamic network coverage,” *IEEE Transactions on Mobile Computing*, vol. 23, no. 5, pp. 5111–5129, 2024.

[22] H. Ibraiwish, M. W. Eltokhey, and M.-S. Alouini, “Energy efficient deployment of vlc-enabled uav using particle swarm optimization,” *IEEE Open Journal of the Communications Society*, vol. 5, pp. 553–565, 2024.

[23] Y. Zhu, M. Chen, S. Wang, Y. Hu, Y. Liu, and C. Yin, “Collaborative reinforcement learning based unmanned aerial vehicle (uav) trajectory design for 3d uav tracking,” *IEEE Transactions on Mobile Computing*, vol. 23, no. 12, pp. 10 787–10 802, 2024.

[24] Y. Lu, Z. Mi, Y. Zhou, D. Wu, and H. Wang, “Research on the 3d deployment of heterogeneous user uav base stations based on voronoi diagram division,” in *2024 6th International Conference on Communications, Information System and Computer Engineering (CISCE)*, 2024, pp. 240–246.

[25] A. M. Said, D. Qiu, H. Mounbla, H. Afifi, and M. Marot, “A novel voronoi based tool to optimize mu-mimo uav placement with sustainable development concerns,” in *GLOBECOM 2024 - 2024 IEEE Global Communications Conference*, 2024, pp. 5199–5204.

[26] Y. Liu, W. Huangfu, H. Zhou, H. Zhang, J. Liu, and K. Long, “Fair and energy-efficient coverage optimization for uav placement problem in the cellular network,” *IEEE Transactions on Communications*, vol. 70, no. 6, pp. 4222–4235, 2022.

[27] L. Spampinato, D. Ferretti, C. Buratti, and R. Marini, “Joint trajectory design and radio resource management for uav-aided vehicular networks,” *IEEE Transactions on Vehicular Technology*, vol. 74, no. 1, pp. 847–860, 2025.

[28] Y. Bai, H. Zhao, X. Zhang, Z. Chang, R. Jäntti, and K. Yang, “Toward autonomous multi-uav wireless network: A survey of reinforcement learning-based approaches,” *IEEE Communications Surveys & Tutorials*, vol. 25, no. 4, pp. 3038–3067, 2023.

[29] A. Andrew, “Another efficient algorithm for convex hulls in two dimensions,” *Information Processing Letters*, vol. 9, no. 5, pp. 216–219, 1979.

[30] S. N. Chiu, D. Stoyan, W. S. Kendall, and J. Mecke, *Stochastic geometry and its applications*. John Wiley & Sons, 2013.



**Chuan-Chi Lai** (Member, IEEE) received the Ph.D. degree in Computer Science and Information Engineering from National Taipei University of Technology, Taipei, Taiwan, in 2017. He was a postdoctoral research fellow (2017–2020) and contract assistant research fellow (2020) with the Department of Electrical and Computer Engineering, National Chiao Tung University, Hsinchu, Taiwan. From 2017 to 2021, he served as an assistant professor at the Department of Information Engineering and Computer Science, Feng Chia University, Taichung, Taiwan.

He is currently an assistant professor at the Department of Communications Engineering, National Chung Cheng University, Chiayi, Taiwan. He is a member of the IEEE Vehicular Technology Society and the IEEE Communications Society. His research interests include resource allocation, data management, information dissemination, and distributed query processing for moving objects in emerging applications such as the Internet of Things, edge computing, and next-generation wireless networks. Dr. Lai received the Postdoctoral Researcher Academic Research Award from the Ministry of Science and Technology, Taiwan, in 2019, Best Paper Awards at WOCC 2021 and WOCC 2018, and the Excellent Paper Award at ICUFN 2015.